



LJMU Research Online

Bosch, MD, Buck, LT and Strauss, A

Perforations in Columbelloid shells: Using 3D models to differentiate anthropogenic piercing from natural perforations

<http://researchonline.ljmu.ac.uk/id/eprint/22949/>

Article

Citation (please note it is advisable to refer to the publisher's version if you intend to cite from this work)

Bosch, MD, Buck, LT and Strauss, A (2023) Perforations in Columbelloid shells: Using 3D models to differentiate anthropogenic piercing from natural perforations. Journal of Archaeological Science: Reports, 49. ISSN 2352-409X

LJMU has developed [LJMU Research Online](#) for users to access the research output of the University more effectively. Copyright © and Moral Rights for the papers on this site are retained by the individual authors and/or other copyright owners. Users may download and/or print one copy of any article(s) in LJMU Research Online to facilitate their private study or for non-commercial research. You may not engage in further distribution of the material or use it for any profit-making activities or any commercial gain.

The version presented here may differ from the published version or from the version of the record. Please see the repository URL above for details on accessing the published version and note that access may require a subscription.

For more information please contact researchonline@ljmu.ac.uk

<http://researchonline.ljmu.ac.uk/>

1 Title: Perforations in Columbelloid shells: Using 3D models to differentiate anthropogenic
2 piercing from natural perforations.

3
4 Authors: Marjolein D. Bosch^{1,2,*}, Laura T. Buck³, Andre Strauss^{4,5}

5
6 ^{1*} Austrian Archaeological Institute – Prehistory, Austrian Academy of Sciences,
7 Hollandstraße 11–13, 1020 Vienna, Austria, Corresponding author: Email:
8 marjolein.d.bosch@gmail.com

9 ² Turkana Basin Institute Ltd, Turkana, Kenya and Turkana Basin Institute, Stony Brook
10 University, N-507 Social and Behavioural Sciences, Stony Brook, NY 11794–4364, US

11 ³ Research Centre in Evolutionary Anthropology and Palaeoecology, School of Biological and
12 Environmental Sciences, Liverpool John Moores University, Byrom Street, Liverpool, L3 3AF

13 ⁴ Museum of Archaeology and Ethnology, University of São Paulo, Av. Professor Almeida
14 Prado 1466, São Paulo, 05508-070, Brazil

15 ⁵ Max Planck Partner Group for Evolutionary Anthropology, University of São Paulo, Rua do
16 Matão 277, 05508-090, São Paulo, Brazil.

17
18 ORCID DMB: 0000-0002-2829-3832 LTB: 0000-0002-1768-9049 AMS: 0000-0002-2336-1381

19
20 Keywords: personal ornaments, shell beads, *Columbella rustica*, micro-CT scans, 3D models,
21 taphonomy, Upper Palaeolithic, Ksâr 'Akil

22
23 Highlights:

24 * New approach aids identification of personal ornaments in the archaeological record

25 * *Columbella rustica* shells were used as beads from the Initial Upper Palaeolithic on

26 * 3D shell thickness models aid distinction of natural from anthropogenic perforations

27 * *Columbella rustica* and *C. adansoni* share overall shell-thickness distribution pattern

28 * Standardisation of perforation size suggests formal bead manufacture at Ksâr 'Akil

29 [Abstract](#)

30 Perforated shells are often used to study socially mediated behaviour in past hunter-
31 gatherer groups. One of the key issues regarding empty shells from beaches or fossil
32 outcrops is determining human agency in the accumulation and modification of an
33 assemblage. Here we investigate anthropogenic mediation in Initial Upper Palaeolithic and
34 Early Ahmarian assemblages of *Columbella rustica* at Ksâr 'Akil (Lebanon). We compare
35 perforations in the archaeological specimens with data from newly gathered Columbelloid
36 modern death assemblages Tenerife (Spain) using three-dimensional shell-thickness models
37 as templates. This approach, using micro-CT scans of pristine shells to map robust and
38 fragile zones on shell outer-surfaces, allows us to contextualise the two datasets within their
39 natural morphology. Our results show that in natural death assemblages the vast majority of
40 perforations occur in structurally weak zones, and their distribution can be explained by
41 shell morphology in combination with predator activity and other post-mortem damage. In
42 our archaeological dataset we found a higher frequency of perforations in more robust
43 zones and a higher uniformity in their location, size and shape. This suggests human
44 mediation in either the selection or manufacture process and indicates that at Ksâr 'Akil *C.*
45 *rustica* were used as beads from as early as the Initial Upper Palaeolithic and throughout the
46 Early Ahmarian. Standardisation in perforation shape, size and distribution have been

47 argued to be indicative of formalised manufacture processes and our results are thus more
48 congruent with intentional bead manufacture than the selection of naturally-holed
49 specimens.

50 Introduction

51 Symbolic behaviour is aimed at sharing information including social conventions, personal
52 and group identity within and between groups (e.g., d'Errico and Stringer 2011). These
53 socially-mediated behaviours strengthen internal group coherence and serve to establish
54 and maintain boundaries with neighbouring groups (e.g., Hodder 1977). Symbolic
55 information can be coded in material culture, for example ethnographic studies show that
56 personal ornaments including scarification, body paint and beadwork, are often used to
57 mark self-identity and group affiliation (e.g., Kuhn and Stiner 2007; Rigaud et al. 2018;
58 Vanharen 2009; Vanhaeren and d'Errico 2006; White 1992). Personal ornaments have often
59 been used to study socially mediated behaviour in the past as they are among the few items
60 across the range of archaeological material culture remains the function of which is entirely
61 symbolic (e.g., d'Errico and Stringer 2011; d'Errico and Vanhaeren 2007; Hovers and Belfer-
62 Cohen 2006; Martínez-Moreno et al. 2010; Micheli 2021; White 2007). In this context there
63 has been an emphasis on basket-shaped shells of the genus *Tritia* (e.g., Bosch et al. 2019;
64 Bouzouggar et al. 2007; d'Errico et al. 2005, 2009; Henshilwood et al. 2004; Vanhaeren et al.
65 2006; Steele et al. 2019) and bivalves of the genus *Glycymeris* (e.g., Bar-Yosef Mayer et al.
66 2009; 2020; Zilhão et al. 2010). Here we investigate anthropogenic mediation in the Initial
67 Upper Palaeolithic and Early Ahmarian assemblages of dove shells (*Columbella rustica*) at
68 Ksâr 'Akil, Lebanon. Columbelloidea are more frequently used for personal adornment in
69 later periods (e.g., Álvarez Fernández 2008, 2016; Álvarez Fernández and Jöris 2008; Bar-
70 Yosef Mayer 1997, 2019a; Cristiani et al. 2014; Kandel et al. 2018; Perles and Vanhaeren
71 2010; Reese 1982; Rigaud et al. 2015), but are also occasionally recovered in early Upper
72 Palaeolithic European and Levantine contexts (e.g., Bosch et al. 2015a; Bar-Yosef Mayer
73 2019a,b, 2020; Marder et al. 2013; Shimelmitz et al. 2018; Stiner et al. 2013; Vanhaeren and
74 d'Errico 2006).

75

76 In the Mediterranean and the northeastern Atlantic Ocean three morphologically very
77 similar species of *Columbella* Lamarck, 1799 are recognised based on genetic data and a
78 single morphological criterion (Moolenbeek and Hoenselaar 1991; Russini et al. 2017).
79 Genetic research suggests that the Macaronesian *Columbella adansoni* Menke, 1853 and
80 the Mediterranean *Columbella rustica* Linnaeus, 1758 are closely related and together form
81 a sister-clade to the West African *Columbella xiphitella* Duclos, 1840 (Russini et al. 2017).
82 The only morphological feature differentiating *C. rustica* from the other two taxa is that it
83 has a so-called paucispiral protoconch, suggesting direct development without a
84 planktotrophic larval state, whereas *C. adansoni* and *C. xiphitella* share a multispiral
85 protoconch indicating that their ontogeny does involve such a larval state (Moolenbeek and
86 Hoenselaar 1991; Russini et al. 2017). In archaeological specimens the apex on which the
87 protoconch is situated is rarely preserved or has been heavily damaged, rendering the three
88 taxa morphologically indistinguishable. Here we base our taxonomic identifications on the
89 proposed geographic separation and previous malacological assessments (Moolenbeek and
90 Hoenselaar 1991; van Regteren Altena 1962; Russini et al. 2017).

91

92 Taphonomic investigations into the Ksâr 'Akil shell assemblage have shown that *Columbella*
93 *rustica* were collected as empty shells after the mollusc had died (Bosch et al. 2015a). One

94 of the key issues in dealing with beach-collected shells is determining human agency in the
95 accumulation and modification of an archaeological assemblage. In broad chronological
96 terms, the archaeological record suggests that during the Levantine Middle Palaeolithic and
97 the onset of the Upper Palaeolithic, shells were purposefully collected (Bar-Yosef Mayer et
98 al. 2020). Fully intact shells may have been pierced to be used as ornaments, whereas
99 naturally perforated shells may have been intentionally collected for the same purpose
100 without the need for further modification before use (e.g., Bar-Yosef Mayer 2005, 2015;
101 Bosch et al. 2019; Stiner et al. 2013; Vanhaeren et al. 2006). Within an archaeological
102 assemblage there is usually a mix of fully intact, perforated and just broken shells. Several
103 authors have suggested that if evidence can be found for the intentional use of some shells,
104 we can assume that all specimens of that taxon were collected for the same purpose (e.g.,
105 Cristiani et al. 2014; Stiner et al. 2013; see also Haynes and Stanford 1984; Lyman 2013). In
106 fact, White (2007) has argued that the occurrence of fully intact shells is indicative of on-site
107 bead manufacture (see also Álvarez Fernández 2008). Identification of human modification
108 of shells into beads is hampered by two things. First there is considerable overlap or
109 equifinality between human-made and natural perforations (d’Errico et al. 1993). For
110 example, direct or indirect percussion damage may look very similar to shell-damage caused
111 by being twirled around in a rocky-shore environment. Second, damage caused by exposure
112 to an active beach environment prior to collection as well as post-depositional alterations
113 may mask traces of use. Therefore, the classification ‘bead’ frequently rests on a range of
114 factors such as the exclusion of (a-)biotic actors, collection for subsistence purposes, signs of
115 manufacture and or use-wear (see for recent reviews Bay-Yosef Mayer and Bosch 2019;
116 Steele et al. 2019). Anthropogenic-mediation may be identified in selection and transport of
117 raw materials, manufacture processes, beadwork composition and use (e.g., Álvarez
118 Fernández 2008; Bouzouggar et al. 2007; Bar-Yosef Mayer 2005; d’Errico et al. 1993; Perlès
119 and Vanhaeren 2010; Rigaud et al. 2019; Taborin 1993; Vanhaeren et al. 2006, 2013).

120
121 Here we divide shell-life into three stages (Fig 1). Stage 1 presents the phase prior to human
122 collection, including the mollusc’s life and the period after its death when the shell is in a
123 beach environment and exposed to various taphonomic agents including bioerosion (e.g.,
124 attacks by crabs, boring sponges and carnivorous molluscs), wave action and abrasion. Stage
125 2 represents the so-called prehistoric use-life, i.e., from human collection to shell discard.
126 During their use-life shells may be preferentially selected based on their appearance, size,
127 and natural perforations, further they may be intentionally perforated and broken during
128 use, lost or discarded. Stage 3 represents the period after discard, i.e., before and after
129 burial in a sedimentary matrix. In stage 3, post-depositional damage may be caused by e.g.,
130 sediment reworking, diagenesis, trampling and rock falls and lead to chemical dissolution,
131 polish, scratches and breakage through crushing. Stage 3 also comprises damage during
132 excavation (e.g., during sieving) and curation (White, personal communication, 2017).

133
134 We investigate traces of human decision-making in stage 2, namely during collection,
135 manufacture, and/or use of perforated shells (e.g., Claassen 1998; Steele et al. 2019).
136 Frequently used avenues to address these questions include comparing thanatocoenoses
137 with archaeological assemblages, as well as technological and use-wear analyses (e.g., Bar-
138 Yosef Mayer et al. 2009; Bouzouggar et al. 2007; d’Errico et al. 2009; Perlès 2016;
139 Vanhaeren et al. 2006). Here we focus on role of shell structure in the shell-piercing process
140 both in human-made and natural contexts. By using shell thickness as a proxy for structural

141 resistance we aim to improve our ability to distinguish natural from human-made
142 perforations. A recent study has shown that in *Tritia gibbosula* damage caused by natural
143 taphonomic processes (i.e., those occurring both in stage 1 and 3) are more frequent in
144 thinner and structurally weaker zones, and that within these zones damage is randomly
145 distributed (Bosch et al. 2019). We assume this also to be the case for *Columbella* spp. If
146 proven correct, any deviation between the modern death and archaeological assemblages
147 likely reflects human involvement during stage 2 of the shell-life through e.g., manufacture
148 (perforation) processes or specimen selection.
149

150 [Material and Methods](#)

151 Following the approach developed in Bosch et al. (2019) we use μ CT (micro computed
152 tomography) data of pristine modern Columbellidae to create virtual models of shell
153 thickness. From these data three-dimensional (3D) virtual models with heat-maps of shell-
154 thickness are derived to better understand the role of shell-structure in relation to shell
155 morphology in both *Columbella rustica* and its sister taxa: *Columbella adansoni*. We show
156 that both taxa display strong similarities in overall morphology and especially in shell-
157 thickness distribution. We then overlie natural perforation damage from two newly
158 collected modern death assemblages stemming from a rocky shore environment (Tenerife,
159 Spain). In this step, we test our predictions regarding the distribution of natural perforations
160 and damage to which shells may be subjected in the above-mentioned stage 1 of the life of
161 the shell. Finally, we compare these data with perforation distributions in archaeological
162 collections from the Initial Upper Palaeolithic and Early Ahmarian of Ksâr 'Akil in an effort to
163 differentiate natural and anthropogenic perforations.
164

165 [A generalised model of shell thickness.](#)

166 Columbellidae are known to adapt to external factors such as wave-action, their littoral
167 position and tidal height as well as temperature and acidic changes which lead to
168 morphological variation (e.g., Chatzinikolaou et al. 2021; Moolenbeek and Hoenselaar 1991;
169 Russini et al. 2017). In any given assemblage therefore, we may expect a fair amount of
170 morphological variation. To investigate this variability and its effect on our shell thickness
171 models we μ CT-scanned shells from two rocky-shores with drastically different energy
172 regimes, namely the eastern Mediterranean (Tripoli, Lebanon) and the Atlantic (Tenerife,
173 Spain). We chose recent non-archaeological specimens instead of seemingly intact
174 archaeological specimens for two main reasons. First, we needed specimens in pristine
175 condition to obtain the most accurate information about shell-structure and thickness.
176 Second, selecting non-archaeological specimens provides the most accurate representation
177 of the species natural state before human collection (i.e., stage 1). Another option would
178 have been to use more or less intact archaeological specimens in an effort to closely mimic
179 the morphology of the prehistoric shells. However, given scarcity of intact specimens and
180 the extent of intra-species variation it is doubtful that this approach would have captured an
181 accurate representation of the morphological range. Moreover, archaeological specimens
182 although seemingly intact may have endured damage, e.g., polish and abrasion, during
183 archaeological use-life and post-depositionally after discard (stages 2 and 3) which would be
184 impossible to disentangle. Instead we opted for a multi-species approach selecting
185 specimens with different apparent morphology to arrive to a generalised model which can
186 be both applied to our modern-death assemblage (*C. adansoni*) as well as to the Ksâr 'Akil

187 assemblages (*C. rustica*). Our virtual models are thus aimed at reflecting average shell-
188 density and showing differences between thinner and thicker zones within a shell, rather
189 than highlighting specific morphological differences such as the shape and attachment of
190 the aperture's shoulder and the height of the spire. We assume therefore that our
191 generalised model is a good basis to compare and contextualise the distribution of damage
192 in both the Tenerife and Ksâr 'Akil assemblages.

193

194 *Micro-CT-scans of recent specimens*

195 Recent Eastern Mediterranean *Columbella rustica* were selected from the collection
196 Mollusca at Naturalis Biodiversity Center (Locality: Tripoli, *RMNH.Mol.203708*). Recent
197 Macaronesian *Columbella adansoni* were selected from the thanatocoenosis: TF1
198 (Tenerife, Spain; personal collection of MDB). Prior to μ CT-scanning specimens were
199 selected for their pristine preservation and damaged specimens (e.g., showing traces of
200 bioerosion, smoothing and abrasion) were avoided. Several specimens were scanned to
201 detect any specimen-specific abnormalities and ensure the resulting virtual models reflect
202 average shell-density. In addition to scanning intact shells, a sample of *C. rustica* (Locality:
203 Tripoli, *RMNH.Mol.203708*) exhibiting boring sponge damage were selected for μ CT-
204 scanning to investigate the effect of this type of damage on shell-robustness. This was done
205 as a high proportion of the archaeological shells from Ksâr 'Akil display boring sponge
206 damage.

207

208 The shells were μ CT-scanned at the Cambridge Biotomography Centre, University of
209 Cambridge, using a Nikon Metrology XT H 225 ST High Resolution Scanner. Scan parameters
210 were optimised for individual scans (voxel size: 0.01–0.03 mm, isotropic). Segmentation and
211 post-processing were done using Avizo 8.1 (Thermo Fisher Scientific - FEI). For more details
212 on the protocol see Bosch et al. (2019). Shell thickness was computed using a scalar field
213 which was then mapped onto the surface using a colour range from blue (thin) to red (thick)
214 with green representing intermediate thickness. The colour range was adjusted to
215 emphasize thickness variation in the areas of interest and is unique to each shell. The final
216 images were obtained in six standardized views, namely dorsal, ventral, both lateral sides,
217 basal, and apical.

218

219 *Modern death assemblages*

220 Two modern death assemblages from rocky shores on Tenerife, Canary Islands, Spain – TF 1
221 and TF 2 - were collected (Fig 2). A survey of multiple rocky shores revealed that *C. adansoni*
222 are most frequent in patches of sandy substrates, which serve as natural traps for (semi-
223)intact specimens. Sporadically, exceptionally large and intact specimens were recovered
224 from both the sandy patches and rocky substrates at the upper limit of the upper intertidal
225 zone. The most time-effective method was to target patches of sandy substrates in the mid
226 to upper intertidal zone at low tide, from which both the modern death assemblages TF1
227 (n=258; search time 30 min) and TF2 (n=91; search time 20 min) were collected. Compared
228 to a thanatocoenosis from an Atlantic rocky shore, an Eastern Mediterranean assemblage
229 would presumably show less damage, due to the reduced zonal amplitude and limited wave
230 action of the Mediterranean Sea, especially on its eastern coast. Using modern death
231 assemblages from a high-energy environment, like the Tenerife beach, amplifies the array of
232 damage that could potentially be observed. The Tenerife thanatocoenoses data, therefore,
233 are ideally suited to investigating the extent of natural damage in relation to shell thickness.

234 Recording perforation damage followed Bouzouggar et al. (2007) which was adapted for
235 *Columbellidae*.

236

237 Archaeological samples

238 The *Columbella rustica* assemblages of Ksâr 'Akil, Lebanon (Layers XXII and XVII; Fig 3) were
239 used as archaeological datasets. Layer XXII is attributed to the Initial Upper Palaeolithic,
240 which dates to >45.900–43.200 calibrated years before present (cal BP). Layer XVII is
241 attributed to the Early Upper Palaeolithic or Early Ahmarian and dates to 43.300–42.800 cal
242 BP (Bosch et al. 2015b; but see Douka et al. 2015 vs. Bosch et al. 2015c).

243

244 Ksâr 'Akil is well-known for its multi-layered Initial and Early Upper Palaeolithic deposits,
245 which are rare in the region and make it, next to Üçağızlı I (Turkey) and Manot (Israel) Caves,
246 one of the key archaeological sites for this period (e.g., Hershkovitz et al. 2015; Kuhn et al.
247 2001; Stiner et al. 2013). The Ksâr 'Akil rockshelter situated about 3 km from the present-
248 day coast. The excavations in the 1930s and 1940s by Ewing and Doherty recovered
249 exceptionally large mollusc assemblage, making it an ideal case-study. The total
250 mollusc assemblage counts 3571 specimens, twelve percent of which (n=429) are beach-
251 collected *C. rustica* (Bosch et al. 2015a; van Regteren Altena 1962). The excavations by Tixier
252 in the late 1960s and 1970s never reached the Initial and Early Upper Palaeolithic deposits
253 and the recovered mollusc assemblage is therefore not included in this study (Inizan and
254 Gaillard 1978; Tixier and Inizan 1981). The studied material is currently housed in the
255 Department of Fossil Mollusca at the Naturalis Biodiversity Center, Leiden, the Netherlands.

256

257 Data recording and statistics

258 Data recording of archaeological and the natural death or thanatocoenoses assemblages
259 employed E4 (freeware: www.oldstoneage.com) and Microsoft Access software packages.
260 All statistical analyses were done in R (version 3.5.0; R Core Team 2018). Graphics were
261 produced using the R package ggplot2 (Wickham 2009). Pearson's chi-squared tests were
262 used to statistically evaluate categorical data and with small sample sizes Monte Carlo
263 simulations (with 10,000 iterations; Patefield 1981) were carried-out to compute the p-value.
264 For continuous data, the Shapiro-Wilk test was used to test for the normality of the
265 distribution. When appropriate t-tests were used, otherwise Mann-Whitney U tests were
266 employed. For comparison of the multiple modern and archaeological *Columbella* spp.
267 assemblages a Kruskal-Wallis test and Wilcoxon signed rank pairwise tests (with adjusted p-
268 values using the Bonferroni correction) were carried out as not all measurements were
269 normally distributed. In all cases, a p-value < 0.05 was considered significant. Outliers in
270 boxplots are defined as $\geq 1.5x$ the inter-quartile range above the upper quartile and $\leq 1.5x$
271 below the lower quartile.

272 Results

273 Figure 4 shows thickness heat-maps of modern pristine *Columbella adansoni* from TF 1 (top)
274 and *Columbella rustica* Tripoli (centre) and a Tripoli specimen that was subject to damage by
275 boring-sponges (bottom). As expected, there is substantial morphological variation between
276 specimens from both localities. Adaptation to a high-energy regime is apparent in the
277 overall squatter appearance of the TF specimen. Also reflected is Russini and colleagues'
278 (2017) diagnosis concerning the length of the body whorl (i.e. $\frac{2}{3}$ of the shell in *C. rustica* and
279 $\frac{3}{4}$ to $\frac{3}{4}$ in *C. adansoni*). Further, our TF specimen shows broad layered spiral whorls, a well-

280 developed aperture and squat shoulder. The Tripoli specimens conversely are more gracile,
281 displaying an elongated spire and siphonal canal. Despite these morphological differences
282 the spatial distribution of shell-thickness appears to follow a more or less identical template.
283 The shells are thickest (coloured red) along the top of the body whorl attaching to the spire,
284 the siphonal canal and the outer lip of the aperture. The spire-whorls are thinner (coloured
285 blue) than the body whorl. The body-whorl gradually gets thinner towards the periphery
286 (widest part) as well as in the direction of growth. Ventrally, this pattern is overlain by a
287 thicker (coloured yellow to orange) patch on the mid-ventral plain.
288

289 Descriptive statistics for three size measurements, i.e., maximum height, maximum
290 diameter and aperture height, for the here studied *Columbella* spp. assemblages are
291 provided in Table 1. All three measurements show a similar pattern. For KSA Layer XXII,
292 maximum height and aperture height could only be measured in two specimens. Thus, to
293 maximise the sample, maximum diameter is chosen as a proxy for shell size and compared
294 here between the assemblages (Fig. 5). Shapiro-Wilk normality tests revealed that maximum
295 diameter in TF1 is not normally distributed (W: 0.93012, $p < 0.001$). A Kruskal-Wallis test
296 shows strong evidence of a significant difference between the mean ranks of at least one
297 pair of assemblages (Kruskal-Wallis $\chi^2 = 76.358$, $p < 0.001$). Wilcoxon signed rank pairwise
298 tests (p-values adjusted using the Bonferroni correction) show that the modern shell
299 assemblages from Tenerife, TF1 and TF2, are not significantly different ($p = 1$), neither are the
300 Ksâr 'Akil assemblages XXII and XVII ($p = 1$). However, both Ksâr 'Akil assemblages differ
301 significantly from both TF1 and TF2 (all p-values are < 0.001). These differences are mainly
302 caused by the presence of smaller specimens in both Tenerife thanatocoenoses, which are
303 outside the range of the Ksâr 'Akil assemblages. Individual larger specimens, falling in the
304 upper half of the Ksâr 'Akil ranges, are present in the TF1 assemblage and probably cause
305 the non-normal distribution of TF1.
306

307 Most natural damage observed in both the modern death and archaeological assemblages,
308 is situated in the thinner parts of the shell (Fig 6). The exception being boring sponge
309 damage, which appears to be randomly distributed on the shell surface. This latter pattern
310 of damage does not usually penetrate the entire shell surface, is evident in all assemblages
311 and visible in the μ CT-model (Fig. 4, bottom). Although, this type of damage weakens the
312 shell-wall it does not lead to perforations large enough to be suitable for suspension,
313 neither is there any indication that these pits and holes were used to puncture the shell
314 during bead-manufacture. In other words, boring sponge damage is randomly distributed
315 and not aligned with larger perforations. Further, in the modern death assemblages, shell
316 damage is mainly restricted to structurally weaker zones, the thin apex being most affected.
317 Damage on the body-whorl, the next weakest zone, centres on the mid dorsal surface which
318 is the most exposed surface of the body-whorl. A similar pattern is seen in thanatocoenosis
319 of other taxa like *Tritia gibbosula* (Bouzouggar et al. 2007). This pattern is observed in both
320 the archaeological and the thanatocoenoses datasets.
321

322 As expected, there are more types of damage in the modern death assemblages than in the
323 archaeological ones. In part, this could be due to more intense wave action in the Tenerife
324 rocky shore environment or to anthropogenic selection of less damaged shells. Apical
325 damage or loss is frequent in both archaeological and modern specimens. The edges of
326 breaks include both smoothed surfaces, likely caused by water erosion, as well as irregular

327 breakage, which could have been caused by wave-action or post-depositional crushing (e.g.,
328 Claasen 1998). In addition, the lack of smaller (e.g., apical) fragments in the Ksâr 'Akil
329 assemblages may be explained by a size-bias due to recovering techniques (e.g., mesh-size
330 for sieving) during the 1930s and 1940s excavation campaigns. Overall, there is a significant
331 difference in the proportion of damaged versus intact shells between the modern-death and
332 archaeological assemblages (Table 2). Equally, the proportion of damage resulting in a
333 perforation is significantly higher in both archaeological assemblages as is the frequency of
334 dorsal perforations that would facilitate suspension (see e.g., Perlès 2016; Stiner et al.
335 2013).

336

337 The perforation location in both archaeological layers is largely restricted to the mid dorsal
338 (dorsal f and j) and ventral (ventral c) planes. Dorsally, the perforations of all assemblages
339 fall in the thinnest (weakest) part of the body whorl. In the archaeological samples the mid
340 dorsal plane is nearly exclusively affected, whereas in the modern death assemblages
341 damage is more evenly distributed throughout the thinnest part of the body whorl. In
342 addition, there is a marked difference in perforation size relative to shell dimension. In the
343 archaeological assemblages, there is a significant dominance of medium-sized (dorsal f) on
344 the mid dorsal plane compared to both smaller (dorsal d) and larger (dorsal j and o) holes
345 (Table 3). Interestingly, the inter-quartile range of the Ksâr 'Akil maximum perforation
346 diameter is much narrower than in the modern-death assemblages even though the latter
347 shells are overall smaller (Fig. 7). This suggesting standardisation in perforation size in the
348 archaeological specimens.

349 Ventral damage is much less frequent overall and does not warrant statistical evaluation of
350 the data. However at face value, ventral perforations follow the dorsal pattern in that there
351 is a larger variation in perforation size in the modern death assemblages. Further,
352 perforations situated in the thicker (orange) zone of the ventral plane are more common in
353 the Ksâr 'Akil assemblages. Large perforations on the ventral plane in the TF assemblages
354 are caused by damage on the thinner surrounding of the mid dorsal plane removing the
355 thicker central part in the process. The small holes observed in various ventral locations in
356 the TF1 assemblages are largely caused by boring sponges and other bioeroders.

357

358 Discussion and Conclusions

359 In this study we used three-dimensional models of shell thickness to shed light on human
360 decision making in archaeological shell assemblages. Our goal was to contribute to a better
361 understanding of whether shell perforations in archaeological contexts are the result of
362 natural or anthropogenic processes. We distinguished three stages in shell use-life, in which
363 perforations can occur: 1) before human collection, 2) the prehistoric use-life, and 3) after
364 discard. We predicted that most natural taphonomic processes (in stages 1 and 3) would
365 affect structurally weak zones to a higher degree than more robust zones and that damage
366 in zones of similar thickness should be randomly distributed. For stage 1 these hypotheses
367 were largely met. Shell damage is mainly restricted to structurally weak zones, albeit with
368 the exception of boring sponge damage which is randomly distributed across the entire shell
369 surface and leaves holes too small to be suitable for suspension. The thinnest part of the
370 shell, the apex, is most affected by damage, followed by the thinner parts on the periphery
371 of the body whorl. Damage within the thinnest zone of the body whorl is more or less
372 evenly distributed. To verify whether our predictions are correct for stage 3 of shell use-life,
373 more experimental data is needed to better understand the damage caused by post-

374 depositional processes and recovery techniques. For example, by burying whole shells and
375 to expose them to trampling, excavation, sieving, and transport.

376

377 Regarding stage 2 damage, our results suggest that *C. rustica* with natural perforations were
378 specifically collected and/or specimens were intentionally pierced to be used as beads.
379 Previous taphonomic investigations have excluded that these shells were transported to the
380 site by animals and geological processes or that they were collected for consumption.
381 Instead, these specimens were collected as empty shells from beaches (Bosch et al. 2015a).
382 Our results show that all Ksâr 'Akil assemblages are significantly different compared to the
383 modern death assemblages. Average shell-size is significantly larger, but falls within the
384 range of their modern beach-collected counterparts. This pattern has been observed for
385 multiple taxa in Palaeolithic, Mesolithic and Neolithic assemblages (e.g., Benghiat et al.
386 2009; Bosch et al. 2019; Perlès 2016; Vanhaeren et al. 2006). For Columbidae it has been
387 suggested that changes in archaeological shell-size are not caused by natural factors – such
388 as changing sea surface temperatures – but by preferential selection seeing as the
389 archaeological specimens do not exceed the maximal dimensions of modern specimens
390 (e.g., Benghiat et al. 2009; Perlès 2016).

391

392 Our results on breakage patterns show that archaeological shells are more commonly
393 broken than beach-collected ones and that shell damage more often results in a
394 perforation. Further, both shell damage and the spatial distribution of holes is less variable
395 in the archaeological shells. Centrally-located perforations both on the mid-dorsal and mid-
396 ventral plain predominate and medium-sized holes (again both dorsally and ventrally) are
397 significantly more frequent. In fact, the medium to large dorsal perforations often observed
398 in archaeological specimens occur in roughly 10% of the TF natural death assemblages
399 versus approximately 70% in the Ksâr 'Akil shells. Perlès (2016) sees a similar pattern in
400 comparing thanatocoenoses data of *C. rustica* from the Eastern Mediterranean with the
401 Upper Palaeolithic to Neolithic assemblages at Franchthi Cave (Greece). Although she
402 reports drastically lower return rates for intact specimens - namely 11 to 80 shells per
403 collector per hour versus 360 and 355 in TF 1 and TF 2 respectively – she reports a low (less
404 than 10%) return rate for specimens with a dorsal perforation suitable for suspension and
405 congruent with the dominant perforation pattern in her archaeological assemblage. Equally,
406 Stiner and colleagues (2013) report a 20% perforation rate for a modern collection of *C.*
407 *rustica* from the beach below Üçağızlı I Cave (Turkey) of which 10% display medium to large
408 dorsal perforations as seen in the Üçağızlı I Cave specimens. In all three thanatocoenoses
409 overall shell damage and breakage patterns, including perforation rates are very similar. For
410 example, Stiner et al. (2013) report a 75% proportion of (semi)-intact specimens versus
411 70%–78% in the Tenerife assemblages and 66%–79% reported by Perlès (2016). These data
412 suggest that 1) breakage patterns in both *C. rustica* and *C. adansonii* thanatocoenoses are
413 comparable and that 2) the few available Eastern Mediterranean Palaeolithic assemblages
414 deviate significantly from a natural distribution. In addition, our three-dimensional shell
415 models show that perforations on the shells' ventral surface are situated in a thicker part of
416 the shell than its surrounding areas i.e., in a zone which we assumed would be less
417 frequently affected by natural damage. Indeed, although medium-size perforations in this
418 thicker zone do occur in the natural TF1 and TF2 datasets, damage in the weaker zones is
419 more abundant. In other words, the perforations in the archaeological *C. rustica* are more
420 uniform in their location and size. This pattern of standardisation would, from an etic point

421 of view, be ideally suited for ornamentation. Not too small to facilitate suspension, not so
422 large that the object loses its original shape and appearance.

423

424 The perforation patterns cannot be explained solely by natural processes. Instead, they
425 suggest that prehistoric humans specifically selected shells with certain perforations or that
426 they pierced them. We argue that the standardisation of perforation diameter (shown by
427 the narrow inter-quartile range) in *C. rustica* is indicative of anthropogenic piercing (e.g.,
428 Stiner et al. 2013). Indeed, standardisation in bead perforation shape, size and distribution
429 have been argued to signify formalised manufacture processes (e.g., d’Errico et al. 1993;
430 Kuhn and Stiner 2007; White 1999, 2007) and our results are thus more congruent with
431 human manufacture processes than solely selection of naturally-holed specimens.

432

433 In the archaeological *C. rustica*, perforation shape is predominantly irregular and the edge
434 appearance may variably be irregular or smoothed. If the Ksâr ‘Akil specimens are indeed
435 anthropogenically pierced as our data suggests, experimental studies suggest that this type
436 of perforation is most likely achieved by direct hard hammer percussion, with or without
437 rotation (e.g., Benghiat et al. 2009; Cristiani et al. 2014; d’Errico et al. 1993; Stiner et al.
438 2013). In relation to the large shell-size, Benghiat et al. (2009) found during their
439 experiments that larger specimens are less likely to shatter during manufacture when using
440 hard hammer percussion. Detailed microscopic analysis of the archaeological assemblage is
441 needed to identify possible traces of manufacture and use-wear, which could confirm or
442 refute the suggestion that direct hard hammer percussion was used to perforate the Ksâr
443 ‘Akil shells.

444

445 Our study adds to a growing body of data using modern death assemblages (e.g.,
446 Bouzouggar et al. 2007; d’Errico et al. 2009; Perlès 2016; Stiner et al. 2013; Vanhaeren et al.
447 2006). We contribute to these studies by providing data on perforation locations in
448 thanatocoenoses of *C. adansonii*, which to our knowledge has not been published before. In
449 addition, the use of our three-dimensional shell models aids to better quantify shell-damage
450 in relation to species-specific shell structures. This approach using micro-CT scans is perhaps
451 most useful in 1) shell assemblages where (post-depositional) taphonomy has obliterated
452 any evidence of bead manufacture and use 2) in cases where both modified and naturally
453 perforated shells were used, and 3) like with the Ksâr ‘Akil *C. rustica*, in instances in which
454 the mode of perforation mimics natural damage processes. In addition, our approach
455 facilitates identification of evidence for standardisation in manufacture processes, which in
456 turn, can help us to better understand socio-economic behaviours underpinning shell bead
457 manufacture and use. Our investigations suggest that in general thin shell-zones are more
458 prone to natural damage than more robust ones. Evaluation of perforation patterns on
459 these templates and especially identifying deviations from the natural patterns provides
460 new insights into human-mediation with *C. rustica* shells during Initial and Early Upper
461 Palaeolithic at Ksâr ‘Akil. Such as evidence for formalised bead manufacture using *C. rustica*
462 as early as the Initial and Early Upper Palaeolithic in the eastern Mediterranean.

463

464 [Acknowledgements](#)

465 We would like to dedicate this paper to Randy White, for his huge contribution to the field
466 of Palaeolithic personal adornment. MDB would like to thank Jeroen Goud, Bram van der
467 Bijl, Frank Wesselingh, and Ronald Pouwer from Naturalis Biodiversity Center, Leiden (NL)

468 for access to the modern and Ksâr 'Akil collections. Carolina Mallol for information of good
469 locations to collect the *Columbella adansoni* assemblages and Philip Nigst for help with its
470 collection and for reading an earlier draft of this paper. We are further indebted to the
471 participants of the HEPO (Tel Aviv) and EU-BEADS (Cambridge) workshops as well as Martin
472 Jones and Jay Stock, for helpful discussions.

473

474 This study has been funded by a H2020 Marie Skłodowska-Curie fellowship ('EU-BEADS',
475 project no. 656325) and a Seal of Excellence Fellowship of the Austrian Academy of Sciences
476 ('TechnoBeads' project no. 101061287) to MDB.

477

478 [References](#)

479

480 Álvarez Fernández, E., 2008. The use of *Columbella rustica* (class: gastropoda) in the Iberian
481 Peninsula and Europe during the Mesolithic and the early Neolithic. In *IV Congreso del*
482 *Neolítico Peninsular: 27–30 de noviembre de 2006*, Hernández Pérez, M.S., Soler Díaz,
483 J.A., and López Padilla, J.A. (eds.). Museo Arqueológico de Alicante-MARQ, Alicante,
484 pp. 103–111.

485 Álvarez Fernández, E., 2016. Souvenirs de la Plage: Les coquillages marins comme preuve
486 der contacts à longue distance des groupes du Paléolithique de la Péninsule Ibérique.
487 Bulletin du Musée d'Anthropologie Préhistorique de Monaco 56, 31–42.

488 Álvarez Fernández, E., Jöris, O., 2008. Personal ornaments in the early upper palaeolithic of
489 Western Eurasia: an evaluation of the record. *Eurasian Prehist* 5(2).

490 Bar-Yosef Mayer, D.E., 1997. Neolithic shell bead production in Sinai. *Journal of*
491 *Archaeological Science* 24(2), 97–111.

492 Bar-Yosef Mayer, D.E., 2005. The Exploitation of Shells as Beads in the Palaeolithic and
493 Neolithic of the Levant. *Paléorient* 31(1), 176–185.

494 Bar-Yosef Mayer, D. E., 2015. Nassarius shells: Preferred beads of the Palaeolithic.
495 *Quaternary International*.

496 Bar-Yosef Mayer, D. E., 2019a. Upper Paleolithic Explorers: The Geographic Sources of Shell
497 Beads in Early Upper Paleolithic Assemblages in Israel. *PaleoAnthropology*, 2019, 105–
498 115.

499 Bar-Yosef Mayer, D.E., 2019b. Mollusk Shells at Kebara Cave. In L. Meignen & O. Bar-Yosef
500 (Eds.), *Kebara Cave, Mt. Carmel, Israel: The Middle and Upper Paleolithic Archaeology:*
501 *Part II* (pp. 403–412). Cambridge, Massachusetts: Peabody Museum of Archaeology and
502 Ethnology, Harvard University.

503 Bar-Yosef Mayer, D. E., 2020. Shell Beads of the Middle and Upper Palaeolithic: A review of
504 the earliest record. In M. Mărgărit & A. Boroneanț (Eds.), *Beauty and the eye of the*
505 *beholder: personal adornments across the millennia* (pp. 11-25). Târgoviște: Cetatea de
506 scaun.

507 Bar-Yosef Mayer, D. E., & Bosch, M. D. (2019). Humans' Earliest Personal Ornaments: An
508 Introduction. *PaleoAnthropology*, 19–23.

509 Bar-Yosef Mayer, D.E., Vandermeersch, B., Bar-Yosef, O., 2009. Shells and ochre in Middle
510 Paleolithic Qafzeh Cave, Israel: indications for modern behavior. *Journal of Human*
511 *Evolution* 56(3), 307–314.

512 Bar-Yosef Mayer, D. E., Groman-Yaroslavski, I., Bar-Yosef, O., Hershkovitz, I., Kampen-
513 Hasday, A., Vandermeersch, B. et al. 2020. On holes and strings: Earliest displays of
514 human adornment in the Middle Palaeolithic. *PloS one*, 15(7), e0234924.

515 Benghiat, S., Komšo, D., Miracle, P.T. (2009). *An experimental analysis of perforated shells*
516 *from the site of Šebrn Abri (Istria), Croatia.*

517 Bosch, M.D., Wesselingh, F.P., Mannino, M.A., 2015a. The Ksâr 'Akil (Lebanon) mollusc
518 assemblage: Zooarchaeological and taphonomic investigations. *Quaternary*
519 *International* 390, 85–101.

520 Bosch, M.D., Mannino, M.A., Prendergast, A.L., O'Connell, T.C., Demarchi, B., Taylor, S.M.,
521 Niven, L., van der Plicht, J., Hublin, J.-J., 2015b. New chronology for Ksâr Akil (Lebanon)
522 supports Levantine route of modern human dispersal into Europe. *Proceedings of the*
523 *National Academy of Sciences* 112(25), 7683–7688.

524 Bosch, M.D., Mannino, M.A., Prendergast, A.L., O'Connell, T.C., Demarchi, B., Taylor, S.M.,
525 Niven, L., Plicht, J.V.D., Hublin, J.-J., 2015c. Reply to Douka et al.: Critical evaluation of
526 the Ksâr 'Akil chronologies. *Proceedings of the National Academy of Sciences* 112(51),
527 E7035–E7035.

528 Bosch, M. D., Buck, L., & Strauss, A., 2019. Location, Location, Location: Investigating
529 Perforation Locations in *Tritia gibbosula* Shells at Ksâr 'Akil (Lebanon) Using Micro-CT
530 Data. *PaleoAnthropology*, 52–63.

531 Bouzouggar, A., Barton, N., Vanhaeren, M., d'Errico, F., Collcutt, S., Higham, T., Hodge, E.,
532 Parfitt, S., Rhodes, E., Schwenninger, J.-L., 2007. 82,000-year-old shell beads from North
533 Africa and implications for the origins of modern human behavior. *Proceedings of the*
534 *National Academy of Sciences* 104(24), 9964–9969.

535 Chatzinikolaou, E., Keklikoglou, K., & Grigoriou, P., 2021. Morphological properties of
536 gastropod shells in a warmer and more acidic future ocean using 3D micro-computed
537 tomography. *Frontiers in Marine Science*, 8, 427.

538 Claassen, C., 1998. *Shells*. Cambridge University Press: Cambridge.

539 Cristiani, E., Farbstein, R., Miracle, P., 2014. Ornamental traditions in the Eastern Adriatic:
540 The Upper Palaeolithic and Mesolithic personal adornments from Vela Spila (Croatia).
541 *Journal of Anthropological Archaeology* 36, 21–31.

542 d'Errico, F., Stringer, C.B., 2011. Evolution, revolution or saltation scenario for the
543 emergence of modern cultures? *Philos Trans R Soc Lond B Biol Sci* 366, 1060–1069.

544 d'Errico, F., Vanhaeren, M., 2007. Evolution or revolution? New evidence for the origin of
545 symbolic behaviour in and out of Africa. In: Mellars, P. (Ed.), *Rethinking the Human*
546 *Revolution*. Cambridge, pp. 275–286.

547 d'Errico, F., Jardon-Giner, P., Soler-Mayor, B., 1993. Critères à base expérimentale pour
548 l'étude des perforations naturelles et intentionnelles sur coquillages. In: *Traces et*
549 *fonction : les gestes retrouvés*. Université de Liege, Liege, pp. 243–254.

550 d'Errico, F., Henshilwood, C., Vanhaeren, M., van Niekerk, K., 2005. *Nassarius kraussianus*
551 shell beads from Blombos Cave: evidence for symbolic behaviour in the Middle Stone
552 Age. *Journal of Human Evolution* 48, 3–24.

553 d'Errico, F., Vanhaeren, M., Barton, N., Bouzouggar, A., Mienis, H., Richter, D., Hublin, J.-J.,
554 McPherron, S.P., Lozouet, P., 2009. Additional evidence on the use of personal
555 ornaments in the Middle Paleolithic of North Africa. *Proceedings of the National*
556 *Academy of Sciences* 106(38), 16051–16056.

557 Douka, K., Higham, T.F.G., Bergman, C.A., 2015. Statistical and archaeological errors
558 invalidate the proposed chronology for the site of Ksar Akil. *Proceedings of the National*
559 *Academy of Sciences*, 112(51), E7034–E7034.

560 Ewing, F.J., 1947. Preliminary note on the excavations at the Palaeolithic site of Ksar' Akil,
561 Republic of Lebanon. *Antiquity* 21(84), 186–196.

562 Ewing, J.F., 1949. The treasures of Ksar' Akil. *Thought* 24, 255–288.

563 Ewing, J.F., 1948. Ksar' Akil in 1948. *Biblica* 29, 272–278.

564 Haynes, G., Stanford, D., 1984. On the Possible Utilization of *Camelops* by Early Man
565 in North America. *Quaternary Research*, 22, 216–230.

566 Henshilwood, C., d'Errico, F., Vanhaeren, M., Van Niekerk, K., Jacobs, Z., 2004. Middle stone
567 age shell beads from South Africa. *Science* 304(5669), 404–404.

568 Hershkovitz, I., Marder, O., Ayalon, A., Bar-Matthews, M., Yasur, G., Boaretto, E. et al., 2015.
569 Levantine cranium from Manot Cave (Israel) foreshadows the first European modern
570 humans. *Nature*, 520(7546), 216–219.

571 Hodder, I., 1977. The Distribution of Material Culture Items in the Baringo District, Western
572 Kenya. *New Series* 12(2), 239–269.

573 Hovers, E., Belfer-Cohen, A., 2006. “Now you see it, now you don't” – modern human
574 behavior in the Middle Paleolithic. In: Hovers E, K. SL (Eds.), *Transitions Before the*
575 *Transition: Evolution and Stability in the Middle Paleolithic and Middle Stone Age.*
576 Springer, New York, pp. 205–304.

577 Inizan, M.-L., Gaillard, J.M., 1978. Coquillages de Ksar-'Aqil: éléments de parure? *Paléorient*,
578 295–306.

579 Kandel, A. W., Bretzke, K., & Conard, N. J., 2018. Epipaleolithic shell beads from Damascus
580 Province, Syria. *Quaternary International*.

581 Kuhn, S. L., & Stiner, M. C., 2007. Paleolithic Ornaments: Implications for Cognition,
582 Demography and Identity. *Diogenes*, 54(2), 40–48.

583 Kuhn, S.L., Stiner, M.C., Reese, D.S., Güleç, E., 2001. Ornaments of the earliest Upper
584 Paleolithic: New insights from the Levant. *Proceedings of the National Academy of*
585 *Sciences* 98(13), 7641–7646.

586 Lyman, R. L., 2013. Paleoindian exploitation of mammals in eastern Washington State.
587 *American Antiquity*, 78(2), 227–247.

588 Marder, O., Alex, B., Ayalon, A., Bar-Matthews, M., Bar-Oz, G., Bar-Yosef Mayer, D. et al.,
589 2013. The Upper Palaeolithic of Manot Cave, Western Galilee, Israel: the 2011–12
590 excavations. *Antiquity*, 87(337).

591 Marean, C.W., Bar-Matthews, M., Bernatchez, J., Fisher, E., Goldberg, P., Herries, A.I.R.,
592 Jacobs, Z., Jerardino, A., Karkanas, P., Minichillo, T., Nilssen, P.J., Thompson, E., Watts, I.,
593 Williams, H.M., 2007. Early human use of marine resources and pigment in South Africa
594 during the Middle Pleistocene. *Nature* 449(7164), 905–908.

595 Martiniz-Moreno, J., Mora, R., Casanova, J., 2010. Lost in the mountains? Marine
596 ornaments in the Mesolithic of the northeast of the Iberian Peninsula. *Munibe*
597 *Suplemento/Gehigarria* 31, 100–109.

598 Micheli, R., 2021. Similarities and Differences Between Italian Early Neolithic Groups: The
599 Role of Personal Ornaments. *Open Archaeology* 7(1), 1274–1294.

600 Moolenbeek, R. G., & Hoenselaar, H. J., 1991. On the identity of 'Columbella rustica' from
601 West Africa and the Macaronesian islands. *Bulletin Zoologisch Museum*, 13(6), 65–70.

602 Patefield, W.M., 1981. Algorithm AS 159: An Efficient Method of Generating Random R × C
603 Tables with Given Row and Column Totals. *Journal of the Royal Statistical Society. Series*
604 *C (Applied Statistics)* 30(1), 91–97.

605 Perlès, C., 2016. Modern reference collections of *Columbella rustica* from Greece. *The*
606 *Arkeotek Journal* 1.

- 607 Perlès, C., Vanhaeren, M., 2010. Black Cyclope neritea marine shell ornaments in the Upper
608 Palaeolithic and Mesolithic of Franchthi Cave, Greece: arguments for intentional heat
609 treatment. *Journal of Field Archaeology* 35(3), 298–309.
- 610 Reese, D. S., 1982. Marine and fresh-water molluscs from the Epipaleolithic site of Hayonim
611 Terrace, Western Galilee, Northern Israel, and other East Mediterranean sites.
612 *Paléorient*, 8(2), 83–90.
- 613 Rigaud, S., d’Errico, F., & Vanhaeren, M., 2015. Ornaments reveal resistance of north
614 European cultures to the spread of farming. *PLoS One*, 10(4), e0121166.
- 615 Rigaud, S., Manen, C., de Lagrán, I.G.-M., 2018. Symbols in motion: Flexible cultural
616 boundaries and the fast spread of the Neolithic in the western Mediterranean. *PloS one*
617 13(5), e0196488.
- 618 Rigaud, S., Costamagno, S., Pétilion, J.-M., Chalard, P., Laroulandie, V., & Langlais, M., 2019.
619 Settlement Dynamic and Beadwork: New Insights on Late Upper Paleolithic Craft
620 Activities. *PaleoAnthropology*, 2019, 137–155.
- 621 Russini, V., Fassio, G., Modica, M. V., deMaintenon, M. J., & Oliverio, M., 2017. An
622 assessment of the genus *Columbella* Lamarck, 1799 (Gastropoda: Columbellidae) from
623 eastern Atlantic. *Zoosystema*, 39(2), 197–212.
- 624 Steele, T. E., Álvarez-Fernández, E., & Hallett-Desguez, E., 2019. A Review of Shells as
625 Personal Ornamentation during the African Middle Stone Age. *PaleoAnthropology*,
626 2019, 24–51.
- 627 Shimelmitz, R., Friesem, D. E., Clark, J. L., Groman-Yaroslavski, I., Weissbrod, L., Porat, N. et
628 al., 2018. The Upper Paleolithic and Epipaleolithic of Sefunim Cave, Israel. *Quaternary*
629 *International*, 464, 106–125.
- 630 Stiner, M.C., Kuhn, S.L., Güleç, E., 2013. Early Upper Paleolithic shell beads at Üçağızlı Cave I
631 (Turkey): technology and the socioeconomic context of ornament life-histories. *J Hum*
632 *Evol* 64(5), 380–398.
- 633 Taborin, Y., 1993. *La parure en coquillage au Paléolithique*. CNRS Editions: Paris.
- 634 Tixier, J., Inizan, M.-L., 1981. Ksar Aqil, stratigraphie et ensembles lithiques dans le
635 Paléolithique Supérieur: fouilles 1971-1975. *Préhistoire du Levant: chronologie et*
636 *organisation de l’espace depuis les origines jusqu’au VI^e millénaire*. Colloques
637 Internationaux du CNRS, 10–14.
- 638 van Regteren Altena, C.O., 1962. Molluscs and Echinoderms from Palaeolithic deposits in
639 the Rock Shelter of Ksâr’Akil, Lebanon. *Zoologische Mededelingen* 38(5), 87–99.
- 640 Vanhaeren, M., d’Errico, F., 2006. Aurignacian ethno-linguistic geography of Europe
641 revealed by personal ornaments. *Journal of Archaeological Science* 33(8), 1105–1128.
- 642 Vanhaeren, M., d’Errico, F., Stringer, C., James, S.L., Todd, J.A., Mienis, H.K., 2006. Middle
643 Paleolithic Shell Beads in Israel and Algeria. *Science* 312(5781), 1785–1788.
- 644 Vanhaeren, M., d’Errico, F., van Niekerk, K.L., Henshilwood, C.S., Erasmus, R.M., 2013.
645 Thinking strings: additional evidence for personal ornament use in the Middle Stone Age
646 at Blombos Cave, South Africa. *J Hum Evol* 64(6), 500–517.
- 647 White, R., 1992. Beyond Art: Toward an Understanding of the Origins of Material
648 Representation in Europe. *Annual Review of Anthropology*, 21, 537-564.
- 649 White, R., 1999. Intégrer la complexité sociale et opérationnelle: la construction matérielle
650 de l’identité sociale à Sungir. In H. Camps-Fabrer (Ed.), *Préhistoire d’os* (pp. 319–333).
651 Provence: L’Université de Provence.
- 652 White, R., 2007. Systems of Personal Ornamentation in the Early Upper Palaeolithic:
653 Methodological Challenges and New Observations. In: Mellars, P., K. Boyle, O. Bar-

654 Yosef, C. Stringer (Eds.), Rethinking the human revolution: new behavioural and
 655 biological perspectives on the origin and dispersal of modern humans. McDonald
 656 Institute for Archaeological Research, University of Cambridge, Cambridge, pp. 287–
 657 302.
 658 Wickham, H., 2009. ggplot2: Elegant Graphics for Data Analysis. Springer: New York.
 659 Zilhão, J., Angelucci, D.E., Badal-García, E., d’Errico, F., Daniel, F., Dayet, L., Douka, K.,
 660 Higham, T.F.G., Martínez-Sánchez, M.J., Montes-Bernárdez, R., Murcia-Mascarós, S.,
 661 Pérez-Sirvent, C., Roldán-García, C., Vanhaeren, M., Villaverde, V., Wood, R., Zapata, J.,
 662 2010. Symbolic use of marine shells and mineral pigments by Iberian Neandertals.
 663 Proceedings of the National Academy of Sciences 107(3), 1023–1028.

664 **Tables and captions**

665
 666 Table 1: Descriptive statistics for *Columbella rustica* from Ksâr ‘Akil (KSA) Layers XXII and
 667 XVII, n: number of specimens, SD: standard deviation.
 668

ID	n	min	max	range	mean	SD
<i>Height max</i>						
KSA-XXII	2	13.71	16.73	3.02	15.22	2.14
KSA-XVII	8	13.81	16.61	2.80	15.21	0.97
TF 1	79	9.09	15.53	6.44	11.88	1.04
TF 2	35	10.53	12.95	2.42	11.40	0.65
<i>Max diameter</i>						
KSA-XXII	11	8.21	11.08	2.87	9.58	0.92
KSA-XVII	29	8.10	10.65	2.55	9.26	0.75
TF 1	142	6.64	10.73	4.09	7.82	0.64
TF 2	62	6.69	9.71	3.02	7.77	0.66
<i>Height Aperture</i>						
KSA-XXII	2	11.14	12.18	1.04	11.66	0.74
KSA-XVII	17	9.81	11.81	2.00	10.63	0.70
TF 1	104	7.14	12.87	5.73	8.93	0.89
TF 2	43	7.66	10.54	2.88	8.85	0.73

669
 670
 671 Table 2: Statistical evaluation of shell damage. *= simulated p-values with 10,000 replicates.
 672

<i>damaged vs intact shells</i>		
	TF1	TF2
KSAXXII	$\chi^2=7.4712$, p=0.005*	$\chi^2=7.1646$, p=0.013*
KSAXVII	$\chi^2=11.536$, p<0.001	$\chi^2=9.809$, p=0.002
<i>damage resulting in a perforation</i>		
	TF1	TF2
KSAXXII	$\chi^2=7.9722$, p=0.005	$\chi^2=13.654$, p<0.001
KSAXVII	$\chi^2=30.287$, p<0.001	$\chi^2=37.582$, p<0.001

dorsal perforation diameter

	TF1	TF2
KSAXXII	$\chi^2=18.305, p<0.001^*$	$\chi^2=15.367, p<0.001^*$
KSAXVII	$\chi^2=41.916, p<0.001$	$\chi^2=25.07, p<0.001^*$

673
674
675
676
677
678

Table 3: Dorsal and ventral shell damage in rocky shore thanatocoenoses from Tenerife (TF1 and TF2) and archaeological assemblages from Ksâr 'Akil (KSA) Layers XXII and XVII. Shell damage in bold, perforation locations in normal font.

	TF1		TF2		KSA XVII		KSA XXII	
	n	%	n	%	n	%	n	%
Beach washed	239	92.64	89	97.80	102	88.70	13	68.42
Dorsal damage	n	%	n	%	n	%	n	%
Not damaged	72	27.52	27	29.67	13	11.30	0	0.00
Damaged	186	72.09	64	70.33	102	88.70	19	100
Damage results in perforation	88	47.31	21	32.81	83	81.37	16	84.21
b - small hole on apex	17	6.54	9	10.11	2	1.26	1	4.00
c - apex gone	85	32.69	30	33.71	62	38.99	8	32.00
d - small hole mid dorsal plain	14	5.38	3	3.37	6	3.77		
e - dorsal side aperture					2	1.26		
f - medium hole mid dorsal plain	15	5.77	1	1.12	60	37.74	13	52.00
h - lateral opposite aperture	3	1.15	1	1.12	1	0.63		
j - large hole dorsal plain	15	5.77	6	6.74	13	8.18	2	8.00
l - aperture broken	40	15.38	14	15.73	12	7.55	1	4.00
m - aperture left	2	0.77						
o - hole all dorsal plain incl apex	29	11.15	1	1.12	1	0.63		
ak - apex left	9	3.46	9	10.11				
an - lateral side left	19	7.31	2	2.25				
ap - body whorl fr	2	0.77	2	2.25				
ar - basal part gone	4	1.54	9	10.11				
as - small hole basal plain	1	0.38	2	2.25				
ao - columella left	5	26.32						
Ventral damage	n	%	n	%	n	%	N	%
Not damaged	258	87.21	87	95.60	106	92.17	18	94.74
Damaged	33	12.79	4	4.40	9	7.83	1	5.26
b - predator hole mid ventral plain					2	22.22		
c - medium hole mid ventral plain centre	6	18.18			6	66.67	1	100
d - small hole on apex			2	50	1	11.11		
e - small hole mid ventral plain centre	3	9.09						

f - small hole mid ventral aperture side	4	12.12		
g - small hole mid ventral opposite aperture	3	9.09		
h - small hole basal plain	1	3.03		
i - all ventral side gone	2	6.06		
j - large hole mid ventral plain aperture side			1	25
k - medium hole mid ventral plain opposite aperture	3	9.09		
l - basal part gone	2	6.06		
m - large hole mid ventral plain	9	27.27	1	25

679

680

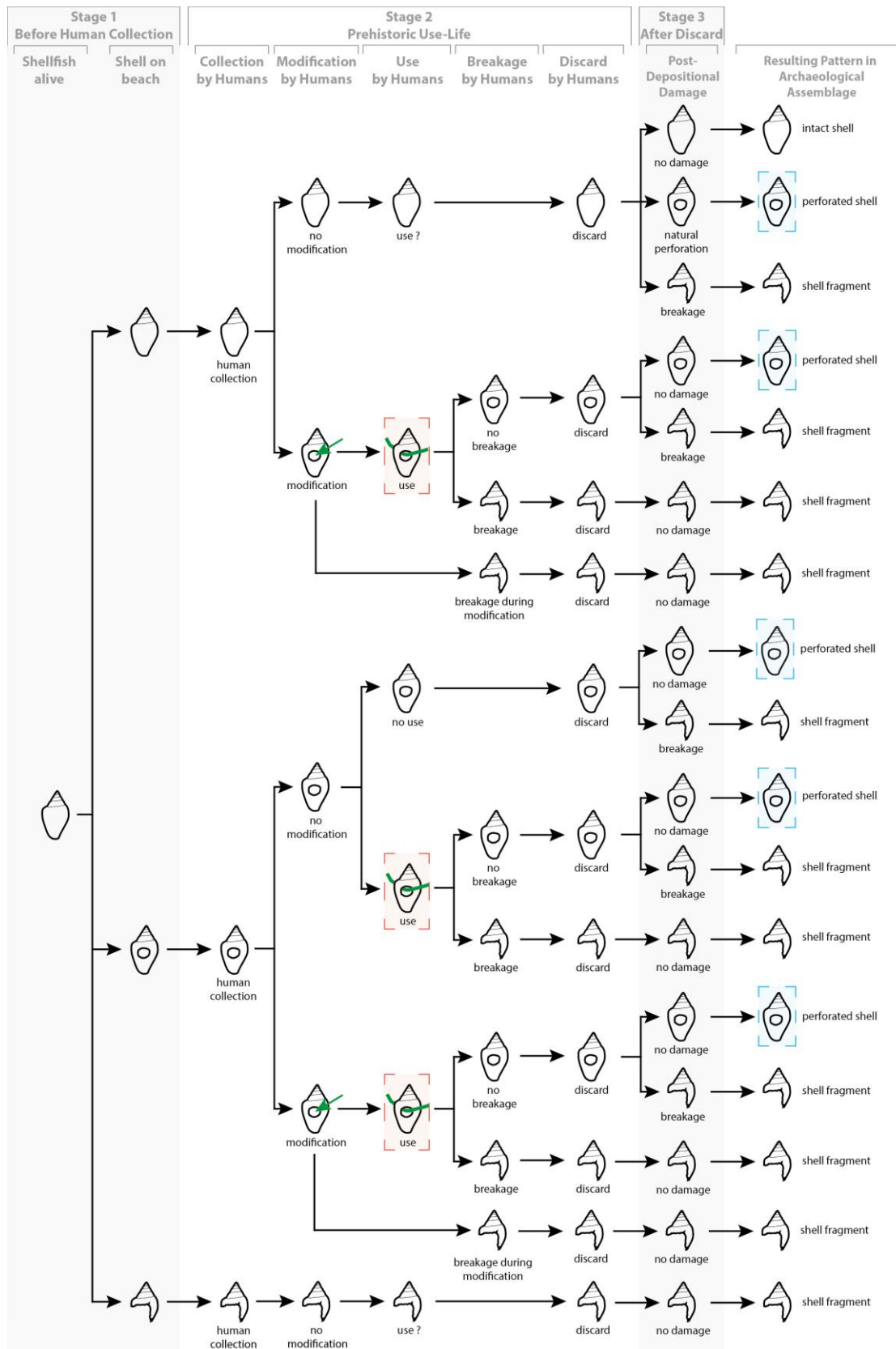


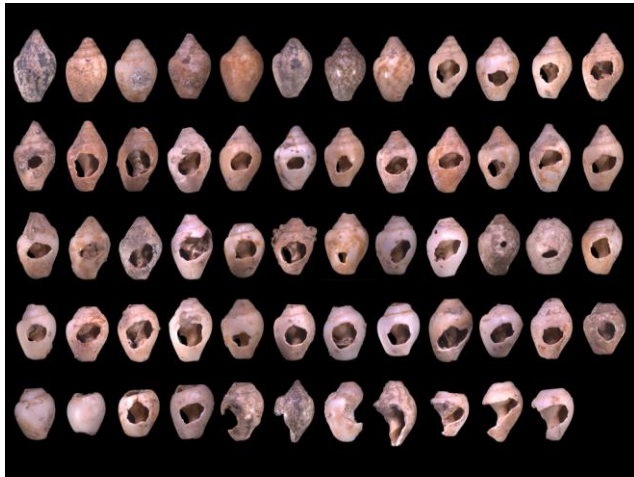
Figure 1. Flow chart showing the use-life of shell specimens found in archaeological assemblages, green arrows: human modifications, red: perforated shells used as beads by prehistoric humans, blue: perforated shells in archaeological record.

687



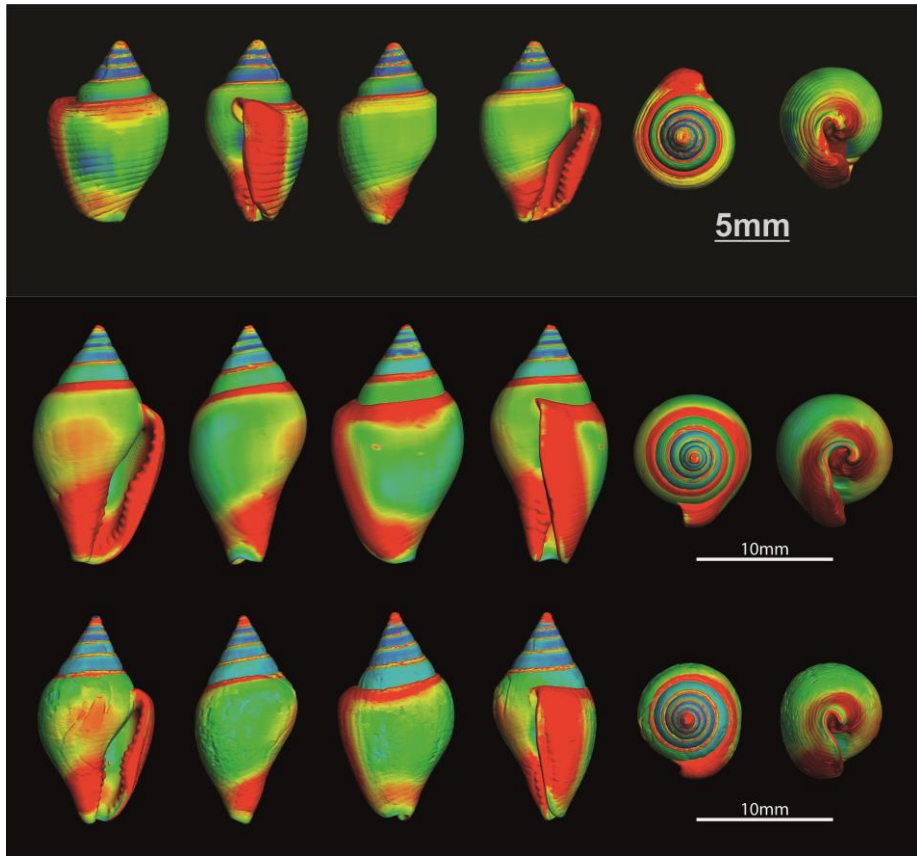
688
689
690
691

Figure 2. Examples of shell damage in *Columbella adansoni* from Tenerife, Spain thanatocoenosis (TF1).



692
693
694
695
696

Figure 3. Examples of shell damage in archaeological specimens of *Columbella rustica* from Ksâr 'Akil, Lebanon Layer XVII (Early Ahmarian).



697

698

699

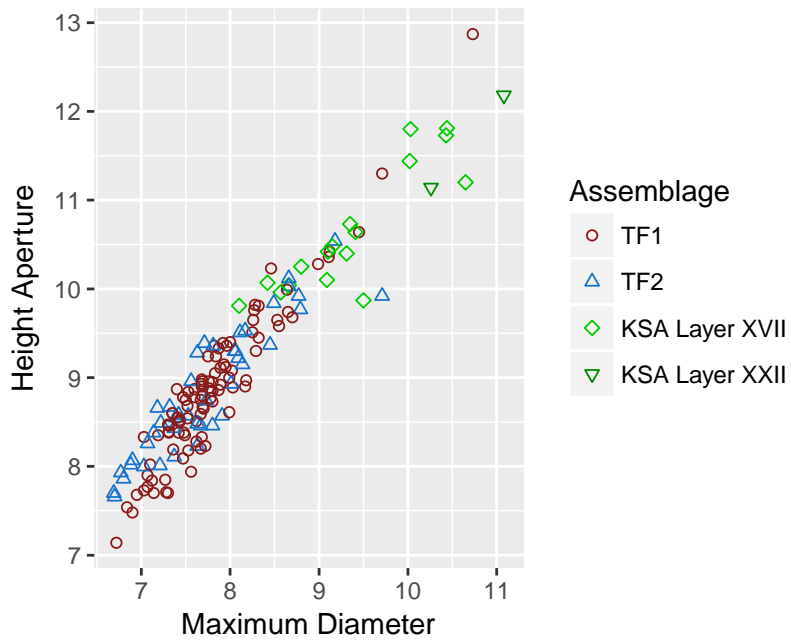
700

701

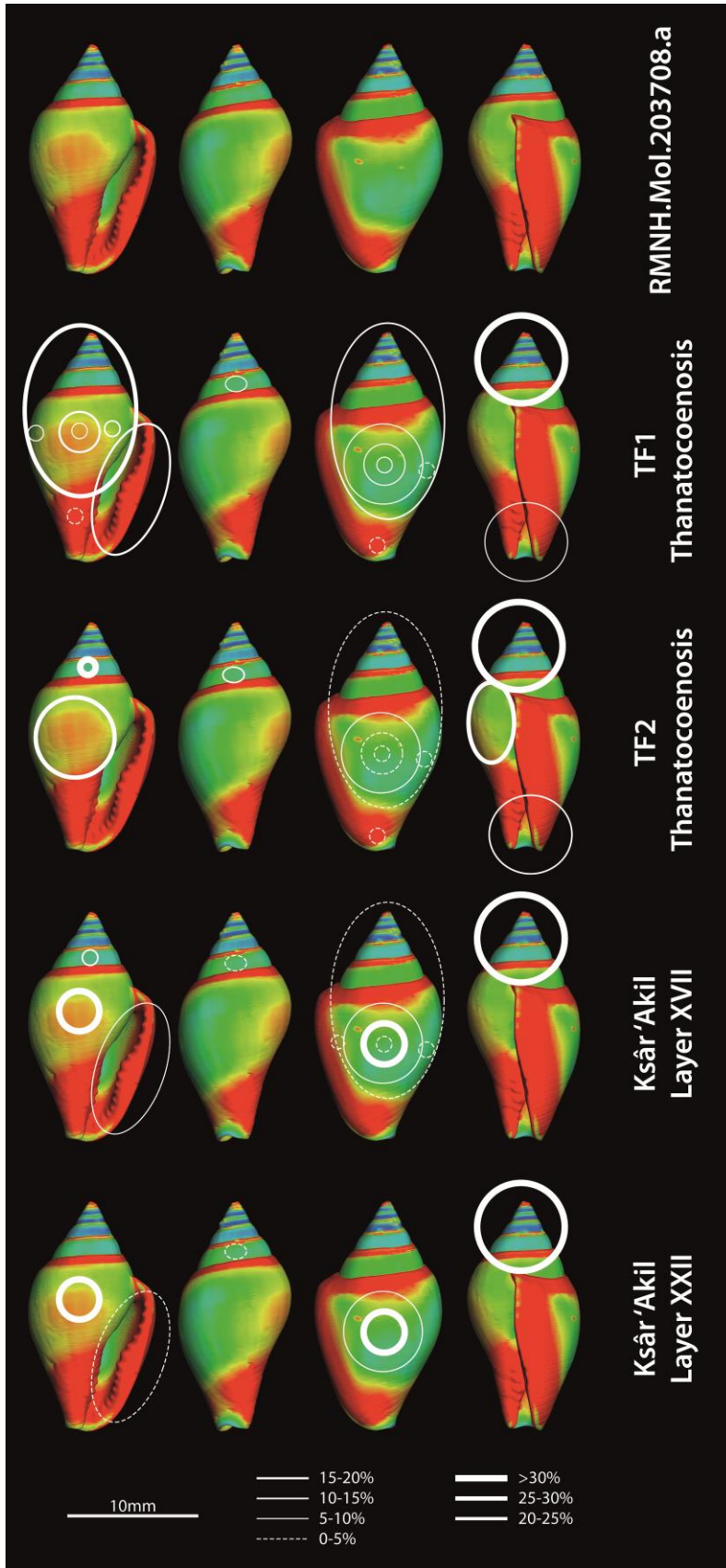
702

703

Figure 4. Heat maps of shell thickness in *Columbella* spp. Top: *Columbella adansoni* from thanatocoenosis (TF1), Middle: pristine *Columbella rustica* (RMNH.Mol.203708.a), bottom: *Columbella rustica* showing boring sponge damage (RMNH.Mol.203708.c). Red to blue: thick to thin.



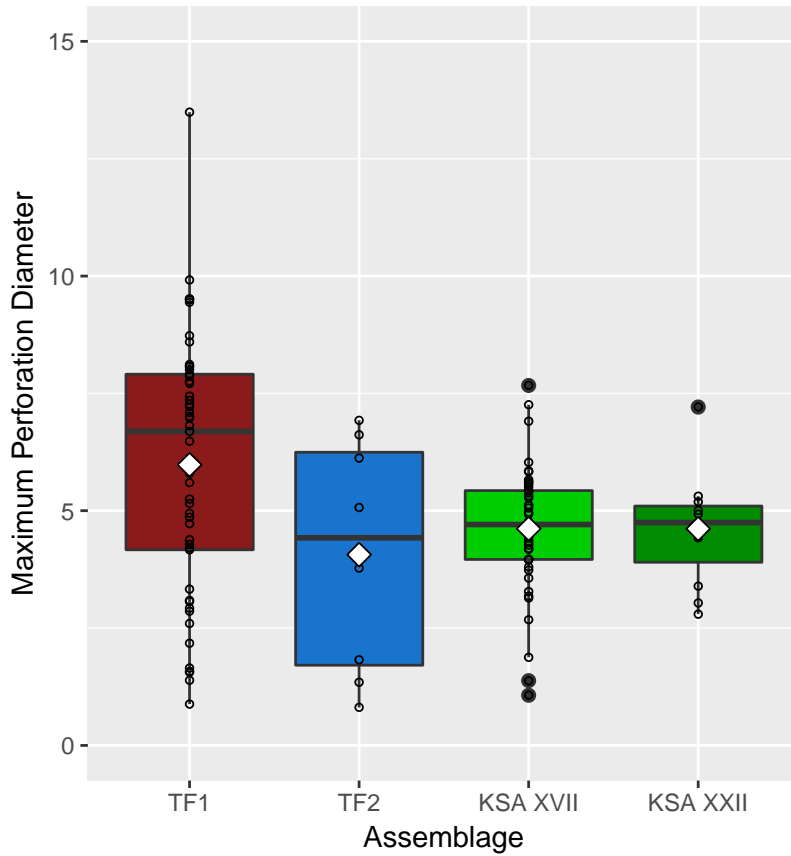
704
 705 Figure 5. Scatterplot comparison of the maximum diameter and the aperture height for
 706 *Columbella rustica* of each analysed assemblage. Tenerife thanatocenooses TF1: red circles,
 707 TF2: blue triangles, Ksâr 'Akil Layer XVII: light green diamonds, Layer XXII: dark green
 708 inverted triangles.



709
710
711
712

Figure 6. Shell damage in *Columbella rustica*, comparing thanatocoenoses TF1 and TF2 with Ksâr 'Akil Layers XXII and XVII. Red to blue: thick to thin. White circles: damaged zones,

713 thickness of line indicates percentage shells damaged in this region (see key in figure). Black
714 circles: perforations by predators.
715



716
717 Figure 7. Boxplots comparing the maximum dorsal perforation diameter for *Columbella*
718 *rustica* between each analysed assemblage. Tenerife thanatocoenoses TF1: red, TF2: blue,
719 Ksâr 'Akil Layer XVII: light green, Layer XXII: dark green. Outliers are shown as solid black
720 circles. Diamonds display the mean.
721